

Forest biomass recovery after different anthropogenic disturbances: relative importance of changes in stand structure and wood density

Dunmei Lin^{1,2,3} · Jiangshan Lai² · Bo Yang^{2,4} · Piao Song² · Ning Li² · Haibao Ren² · Keping Ma²

Received: 4 December 2014 / Revised: 27 April 2015 / Accepted: 4 May 2015
© Springer-Verlag Berlin Heidelberg 2015

Abstract Restoring the functions of disturbed forest to mitigate climate change is a main topic of policy makers. Better understanding of factors that directly influence post-disturbance forest biomass recovery is urgently needed to guide forest restoration and management. In this study, we examine changes in forest stand structure, wood density and biomass of forests recovering from different anthropogenic disturbances that represent forest land-use types in subtropical China: plantation, twice-logged and once-logged secondary forests, and compare them with undisturbed old-growth forest. Stand structure and wood density in all disturbed forests were evidently different from that of old-growth forest, even after 50-year regrowth. Forest biomass increased along plantation, twice-logged, once-logged and old-growth forests, with total living biomass (TLB) ranging from 150.8 ± 4.6 to 278.4 ± 1.5 Mg ha⁻¹, aboveground

biomass from 111.8 ± 4.2 to 204.1 ± 1.5 Mg ha⁻¹ and coarse-root biomass from 33.0 ± 0.9 to 71.0 ± 0.8 Mg ha⁻¹. However, fine-root biomass was highest in plantation (5.99 ± 0.52 Mg ha⁻¹) and lowest in once-logged forest (3.35 ± 0.19 Mg ha⁻¹). Both changes in stand structure and functional trait (wood density) directly determine forest biomass recovery according to the result that 10.6, 35.5 and 8.2 % of variation in TLB over the disturbance gradient were independently explained by basal area (<20 cm diameter), basal area (≥ 20 cm diameter) and wood density, respectively. Our results suggest that recovery forest structure to the state associated with undisturbed forests will lead to large carbon sink in disturbed forests. In addition, trait-based managing approach should not be overlooked when maximizing carbon storage is a major management objective.

Communicated by Aaron R Weiskittel.

Electronic supplementary material The online version of this article (doi:10.1007/s10342-015-0888-9) contains supplementary material, which is available to authorized users.

✉ Dunmei Lin
lindunmei@cqu.edu.cn

¹ Key Laboratory of the Three Gorges Reservoir Region's Eco-Environment, Ministry of Education, Chongqing University, Chongqing 400045, China

² State Key Laboratory of Vegetation and Environmental Change, Institute of Botany, The Chinese Academy of Sciences, Beijing 100093, China

³ National Centre for International Research of Low-Carbon and Green Buildings, Chongqing University, Chongqing 400045, China

⁴ Key Laboratory of Resource Plant and Biotechnology, Jingdezhen University, Jingdezhen 333000, Jiangxi, China

Keywords Anthropogenic disturbance · Subtropical forest · Forest recovery · Forest structure · Wood density

Introduction

Forests are one of the most important terrestrial ecosystems on earth, which provide ecological, economic, social, aesthetic and other services to human beings (MEA 2005; FAO 2010). Forests play an important role in global carbon balance (Houghton 2007; Pan et al. 2011). Regrettably, primary forests are decreasing at an unprecedented rate due to multiple anthropogenic disturbances, resulting in the secondary and planted forests rapidly becoming common land-cover types around the world (FAO 2010).

Better understanding the trajectories of ecological changes in human disturbed forest to recover ecosystem

functions is important for robust and effective climate change mitigation in ecosystem management. Forest recovery following disturbance is a complex process depending on a multitude of factors, such as disturbance type and intensity, climate, soil fertility and availability of seed sources (Guariguata and Ostertag 2001; Chazdon 2003; Chazdon et al. 2007). The degree and speed of disturbed forests recovery following disturbance will determine their values in provision of ecosystem functions. Rate and extent of recovery, however, vary considerably, depending on type and intensity of disturbances, and which forest attributes are being measured (Guariguata and Ostertag 2001; Chazdon et al. 2007; Martin et al. 2013). Forest stand structure, such as stem density and basal area, generally recovers rapidly following disturbance. In contrast, species composition generally recovers more slowly than stand structure (Chazdon et al. 2007; Marin-Spiotta et al. 2007). Both changes in stand structure and functional characteristics of the constituent species may influence recovery of ecosystem functions (Bunker et al. 2005; Díaz et al. 2007; Conti and Díaz 2013).

Wood density is a key functional trait in forests, which strongly correlates with life history strategies of tree species (Chave et al. 2006, 2009). Wood density also strongly correlates with the density of carbon per unit volume and hence partly determines forest biomass and ecosystem carbon stock (Muller-Landau 2004; Chave et al. 2005). For example, forest biomass is higher in regions characterized by higher community wood density in Amazonian tropical forests (Baker et al. 2004; Malhi et al. 2006; Quesada et al. 2012). Similarly, Baraloto et al. (2011) found a positive relationship between forest biomass and stand average wood density in different habitat types. Via simulation analyses, Bunker et al. (2005) reported that replacing species with the lowest wood density by other tree species in a tropical forest can lead to 75 % increases in carbon storage. However, the relative importance of wood density in determining the forest biomass recovery following disturbance has seldom been tested directly.

As one of the typical terrestrial biomes on earth, the subtropical evergreen broad-leaved forest covers an extensive part of China (Wu 1980; Kira 1991), playing an important role in regional and global carbon balance (Fang et al. 2001; Piao et al. 2009). Due to the land-use change and large demand for natural resources associated with the huge population size, large areas of primary evergreen broad-leaved forests have been substantially over-exploited and converted to secondary forests and plantations (Li 2004; Wang et al. 2007). It has been reported that forests in China function as a large carbon sink (Piao et al. 2009; Pan et al. 2011), especially the subtropical forests in south China (Piao et al. 2009). But current carbon sink was primarily caused by increasing forest area associated with the

intensive national afforestation/reforestation programs in the past few decades (Fang et al. 2001; Piao et al. 2009; Pan et al. 2011). Increasing forest biomass density of the existing forests may determine the carbon sink in the future (Canadell and Raupach 2008). With the aim of facilitating the biomass recovery of the existing degraded forests, it is important to identify change in which forest attributes directly related to the variation of biomass among forests with different disturbance or management histories. In addition, the majority of research on post-disturbance forest biomass recovery, however, has had an aboveground focus; as a result, our understanding of the trajectory of belowground biomass recovery is less well known.

In this study, we use a plot network (12 1-ha plots) established along a visible disturbance gradient (Xu et al. 2014), representing forest land-use types in subtropical region of China, to examine following questions: (1). Are the legacies of past disturbance on forest structure and community-weighted mean (CWM) wood density still visible? (2). How does living biomass vary along the disturbance gradient? (3). How much of the variation in biomass along the disturbance gradient is due to variation in forest structure (caused by tree recruitment, growth and mortality) and how much is due to variation in CWM wood density (caused by differences in species composition and their abundance and dominance patterns)?

Materials and methods

Study site

Our study area is located in Gutianshan National Nature Reserve, southeast China (29°10'19.4"–29°17'41.4"N, 118°03'49.7"–118°11'12.2"E; 8107 ha). This place is characterized by subtropical monsoon climate, with a mean annual temperature of 15.3 °C and a mean annual precipitation of 1964 mm (Yu et al. 2001). The parent rock of the mountain range is granite, with soil pH ranging from 5.5 to 6.5 (Lou and Jin 2000). The predominant vegetation type is typical subtropical evergreen broad-leaved forest dominated by *Castanopsis eyrei* (Fagaceae) and *Schima superba* (Theaceae) (Yu et al. 2001). The landscape matrix consists of primary forest surrounded by secondary forest and plantation at different stages of recovery (Yu et al. 2001). A total of 1426 seed-plant species of 648 genera and 149 families have been recorded as native species in this place (Lou and Jin 2000).

In 2009, twelve 100 m × 100 m (1-ha) permanent plots that represented different degrees of disturbance were established within the nature reserve (Xu et al. 2014). Land-use (or disturbance) histories of the 12 study plots were obtained by means of interview with

elderly and official local inhabitants and look up local Forestry Chorography. Three plots were sampled for each forest type. The Chinese fir (*Cunninghamia lanceolata*) plantation, located in the experiment zone of the nature reserve, was planted about 20 years ago. The experiment zone was covered by evergreen broad-leaved forest before 1980s (Editorial Group of Forestry Chorography in Kaihua County 1988). The secondary forests, located in the buffer zone of the nature reserve, were the result of deforestation and natural recovery without other land use: The once-logged forest was clear cut 50 years ago, and the twice-logged forest was clear cut 50 years ago and high-intensive selective logging about 20 years ago. The interval for two logging in the twice-logged forest is about 30 years, and large trees were harvested for timber production and small trees were harvested for firewood during the high-intensive selective logging. The old-growth forest, located in the core zone of the nature reserve, has never been affected by major human disturbance for at least 100 years. Twice-logged, once-logged and old-growth forests together were referred as natural forests henceforth for simplicity. All plots were similar in topography, reducing the probability of differences between plots prior to human disturbances (Xu et al. 2014).

Stand variables characterization

We performed a standard forest census for each 1-ha plot following the main principles of Condit (1998) in 2009. All trees with diameter at breast height (DBH) ≥ 1 cm were measured, tagged, mapped and identified to species. We use basal area and stem density to describe forest stand structure of the four forest types. Basal area was calculated by summing the cross-sectional area of each stem at breast height including the secondary stems that branched from the main stem below breast height (Lin et al. 2012). CWM wood density was calculated as the sum of the species wood density weighted by basal area (Baker et al. 2004) with the following equation:

$$\rho_p = \frac{\sum_{i=1}^{S_p} BA_i \times \rho_i}{\sum_{i=1}^{S_p} BA_i}$$

where ρ_p is the CWM wood density of plot p , ρ_i is the species-specific wood density of species i , BA_i is the basal area of species i in plot p , and S_p is the number of species in plot p . Species-specific wood density values were obtained for each tree species from Liu et al. (2012) measured within the nature reserve. In cases where wood density value was unavailable for a particular species (only few uncommon species), a genus-level or a family-level mean value was taken (Chave et al. 2006).

Living biomass estimation

Stand inventories were converted to aboveground biomass (AGB) using published allometric equations (Table 1). All species-specific equations used in this study were derived from study areas with similar climate. 79 ± 14 % (mean ± 1 SD) of the basal area of each 1-ha plot was covered by species-specific allometric equations. All of the species that did not have species-specific allometric equation are broad-leaved trees, and their AGB was calculated by using the pan-tropical allometric equation of Chave et al. (2005) for moist tropical forests after considering the bioclimatic conditions of our study site:

$$AGB = 0.0509 \times \rho D^2 H$$

where AGB is aboveground dry biomass in kg, ρ is species-specific wood density (g cm^{-3}) as described above, D is DBH (cm), and H is tree height (m). We tested the applicability of this allometric equation to our study site by using a small sample of trees ($n = 69$; 12 species) harvested near the study site. The biomass values were not significantly different from the predictions of Chave's equation (mean difference = 3.65 kg, bootstrapped 95 % confidence intervals $[-3.25, 9.85]$ including zero). Tree height was determined via 48 species-specific and one general regression models developed from a sample of 1066 trees measured by Lin et al. (2012) within the nature reserve and 32 trees (for *C. lanceolata*) measured in the plantation in this study. All of the tree height regression models used in this study can be found in Table S1. For coarse-root biomass (CRB), allometric equations were built with raw harvest data previously acquired in the nature reserve (Lai et al. 2013) and Xingangshan, ~ 15 km from the nature reserve (Li et al. 2013). Species-specific equations were developed for the two conifer species (*P. massoniana*, *C. lanceolata*) and the two most dominant broad-leaved tree species (*C. eyrei* and *S. superba*), and a general equation was developed for other broad-leaved tree species. Modeling procedure and model selection were similar to the methods of Chave et al. (2005). Finally, we used the following allometric equations for individual trees to convert the inventory data into CRB:

P. massoniana ($n = 58$, $R^2 = 0.98$, DBH range: 1.3–56.5 cm):

$$CRB = \exp\left(-4.27532 + 1.66537 \ln(D) + 0.58447(\ln(D))^2 - 0.09286(\ln(D))^3\right) \times 1.053685$$

C. lanceolata ($n = 17$, $R^2 = 0.94$, DBH range: 1.0–22.3 cm):

$$CRB = \exp\left(-1.4312 + 0.52796(\ln(D))^2\right) \times 1.06892$$

Table 1 Species-specific allometric equations for aboveground biomass estimation in this study

Species	Species-specific allometric equations	R^2	References
<i>Schima superba</i>	$AGB = 0.07103 (D^2H)^{0.91}$	0.96	Zhang et al. (2007)
<i>Pinus massoniana</i>	$AGB = 0.13529 (D^2H)^{0.79}$	0.91	Zhang et al. (2007)
<i>Cyclobalanopsis glauca</i>	$AGB = 0.08542 (D^2H)^{0.91}$	0.93	Zhang et al. (2007)
<i>Cunninghamia lanceolata</i>	$AGB = 0.11584 (D^2H)^{0.75}$	0.94	Zhang et al. (2007)
<i>Castanopsis carlesii</i>	$AGB = 0.0453 D^{1.716} + 0.037 D^{2.4599} + 0.1565 D^{2.2772}$	>0.98	Yang et al. (2010)
<i>Cyclobalanopsis myrsinaefolia</i>	$AGB = 0.1019 \exp(0.1387 D) + 0.0358 D^{2.4556} + 0.3152 D^{2.016}$	>0.96	Yang et al. (2010)
<i>Castanopsis eyrei</i>	$AGB = 0.06491 (D^2H)^{0.92}$	0.98	Du et al. (1987)
<i>Lithocarpus glaber</i>	$AGB = 0.04268 (D^2H)^{0.98}$	0.99	Du et al. (1987)
<i>Alniphyllum fortune</i>	$AGB = 0.8003 (D^2H)^{0.5276} + 0.1768 (D^2H)^{0.5648} + 0.564 (D^2H)^{0.3191}$	>0.95	Chen (2000)
<i>Loropetalum chinense</i>	$AGB = 0.1599 \times D^{2.35119}$	0.99	Lin et al. (2012)
<i>Rhododendron ovatum</i>	$AGB = 0.3323 \times D^{1.7874}$	0.96	Lin et al. (2012)
<i>Rhododendron latoucheae</i>	$AGB = 0.2212 \times D^{1.9932}$	0.92	Lin et al. (2012)

AGB aboveground dry biomass (kg), D diameter at breast height (cm), H tree height (m)

C. eyrei ($n = 41$, $R^2 = 0.98$, DBH range: 1.1–47.0 cm):

$$CRB = \exp\left(-1.7237 + 1.08179 (\ln(D))^2 - 0.15736 (\ln(D))^3\right) \times 1.044937$$

S. superba ($n = 62$, $R^2 = 0.97$, DBH range: 1.2–38.3 cm):

$$CRB = \exp\left(-1.80254 + 1.14492 (\ln(D))^2 - 0.16527 (\ln(D))^3\right) \times 1.086219$$

Other broad-leaved species ($n = 204$, $R^2 = 0.96$, DBH range: 1.1–47.0 cm):

$$CRB = \exp(-0.47804 + 1.03859 (\ln(D))^2 - 0.14075 (\ln(D))^3 + 1.89538 \ln(\rho)) \times 1.07776$$

where CRB is coarse-root biomass (kg), D is DBH (cm), ρ is species-specific wood density (g cm^{-3}) as described above, \ln is natural logarithm, and \exp is exponential function.

Fine-root biomass (root <2 mm in diameter; FRB) was determined in each plot by core sampling in August 2011. The sampling tool is a sharp-edged metal cylinder with an inner diameter of 10 cm. We designed 72 sampling points for each plot, i.e., 36 fixed points in the intersection points of the 20 m \times 20 m grid in each 1-ha plot and 36 random points along a random compass direction (N, E, S, W, NE, NW, SE or SW) of each fixed point (Fig. 1a). However, during the field work, we found that it is time-consuming and laborious to process the soil samples. In addition, large sampling is also destruction to the forest plots which are established for long-term forest dynamic monitoring. Accordingly, we carried out the original design only in one plot of the twice-logged, once-

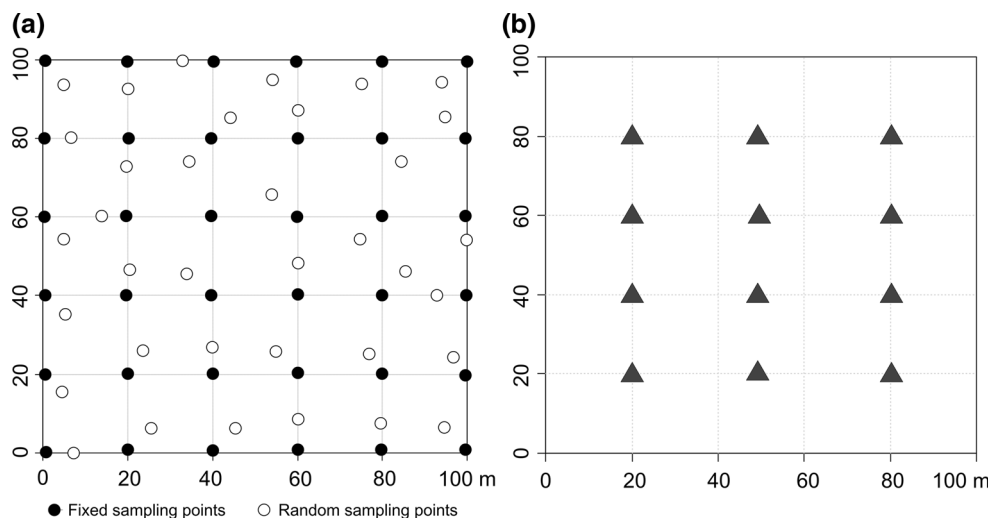
logged and old-growth forests. For other plots, only the 36 fixed points and a few random points were sampled. Finally, 37–72 sampling points were selected for a 1-ha plot. The soil samples were taken at 10-cm intervals down to the depth of 60 cm (including the organic layer) for each sampling point. The soil samples were transferred to polyethylene bags and transported to the laboratory. In laboratory, soil samples were soaked in water and the fine roots were manually separated from soil by sieving and washing (Oliveira et al. 2000). Coarse roots (>2 mm diameter) and coarse fragments were removed. Dead and live fine roots were separated during the sieving procedure based on physical appearance and structural integrity (Oliveira et al. 2000). The living fine roots were oven-dried at 85 °C to a constant weight and weighed. FRB of each plot was calculated using the following equation:

$$FRB_p = \frac{\sum_{i=1}^n \sum_{j=1}^l \frac{4m_{ij}}{\pi}}{n}$$

where FRB_p is the fine-root biomass of plot p (Mg ha^{-1}), n is the number of sampling point in plot p , l is the number of sampling layer of the sampling point i , and m_{ij} is the fine-root biomass in the layer j of the sampling point i (g).

Total living biomass (TLB) was calculated as the sum of AGB, CRB and FRB for each plot. In addition, we estimated average biomass recovery rate for disturbed forests via dividing the biomass by the time (number of year) since last disturbance. However, for the twice-logged forest, some trees may survive after the high-intensive selective logging, which is likely to lead to slight overestimation in average recovery rate of living biomass. Consequently, we also calculated the adjusted biomass recovery rate by

Fig. 1 Sampling design for fine-root biomass estimate (a) and soil data collection (b) in each 1-ha plot



assuming that trees with $DBH \geq 30$ cm were the survivals of the past selective logging for the twice-logged forest.

Environmental variable characterization

In April 2011, 12 soil cores were taken to a depth of 15 cm for each 1-ha plot (Fig. 1b). Soil samples were air-dried and put through a 2-mm sieve to remove roots and stones. In laboratory, two chemical variables (total organic carbon, total nitrogen) and soil texture (percentage of sand, clay and silt) were determined for each soil sample following the methods described in Du and Gao (2006). Values for the 12 soil samples per plot were averaged before statistical analysis.

Statistical analysis

One-way analysis of variance (ANOVA) was used to test for significant differences in stand structure, CWM wood density and forest living biomass among the four forest types, and Tukey's post hoc tests were used to evaluate the significance of differences between each pair of them. With the goal to determine how much of the variation in living biomass could be explained by changes in stand structure and CWM wood density, we built multiple linear regression models considering stem density ($DBH < 20$ cm), stem density ($DBH \geq 20$ cm), basal areal ($DBH < 20$ cm), basal areal ($DBH \geq 20$ cm) and CWM wood density as explanatory variables, and TLB, AGB, CRB and FRB as response variables, respectively. In order to account for the possible influence of environmental factors, soil variables were also added to the regression models. We used principal components analysis (PCA) to reduce the strong collinearity observed among soil variables and extracted the first three principal components as environmental factors in our study, which capturing 99.7 % of the variation in these soil variables (PC1 = 53.3 %, PC2 = 30.1 %, PC3 = 16.3 %;

Table S2). Akaike information criterion (AICc, corrected for small sample sizes) was used to determine the best-fit models (Burnham and Anderson 2004). Variables were eliminated from the full model until a minimal, best-fit model with the lowest global AICc was obtained (Burnham and Anderson 2004). In order to quantify the various unique and combined fractions of the variation in response variables explained by each explanatory variable retained in the best fitted model, partial regression analysis was used (Legendre and Legendre 2003).

Results

Changes in forest stand variables

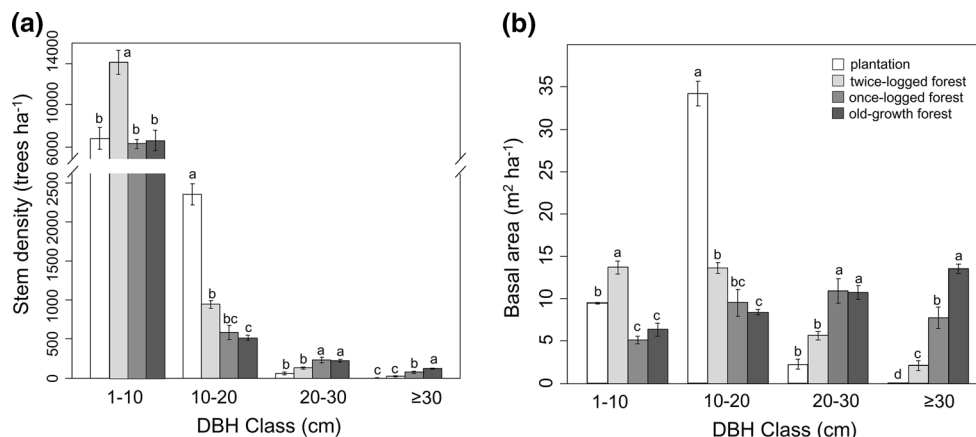
Stem density was significantly higher in the twice-logged forest compared to other forest types ($15,202 \pm 1123$ trees ha^{-1} ; $P < 0.001$), and the lowest stem density was observed in once-logged forest (7221 ± 359 trees ha^{-1} ; Table 2). Twice-logged forest had significantly more small trees (1–10 cm DBH) than any of the other forest types ($14,110 \pm 1175$ trees ha^{-1} ; $P < 0.001$; Fig. 2a), while plantation had significantly more individuals in the size class 10–20 cm DBH than any of the other forest types (2352 ± 139 trees ha^{-1} ; $P < 0.0001$; Fig. 2a). Stem density of the once-logged and old-growth forests in the large size classes (≥ 20 cm DBH) was significantly higher than that of twice-logged forest and plantation (Fig. 2a). Significant difference in stem density between once-logged and old-growth forests was only observed in the largest size class (≥ 30 cm DBH) (75 ± 14 vs. 119 ± 2 trees ha^{-1} ; $P = 0.013$; Fig. 2a). Plantation had the highest basal area (46.03 ± 1.73 m^2 ha^{-1}), even higher than that of the old-growth forest (39.08 ± 1.69 m^2 ha^{-1} ; $P = 0.112$) and significantly higher than that of once- and twice-logged forests ($P = 0.006$ and 0.014 , respectively; Table 2). Size distribution

Table 2 Stand variables of the four forest types in this study

Forest type	Stem density (trees ha ⁻¹)	Basal area (m ² ha ⁻¹)	CWM wood density (g cm ⁻³)
Plantation	9274 ^b ± 913	46.03 ^a ± 1.73	0.377 ^c ± 0.004
Twice-logged	15202 ^a ± 1123	35.09 ^b ± 1.57	0.531 ^b ± 0.001
Once-logged	7221 ^b ± 359	33.40 ^b ± 2.39	0.546 ^{ab} ± 0.002
Old-growth	7513 ^b ± 1041	39.08 ^{ab} ± 1.69	0.576 ^a ± 0.013

Values are mean ± SE ($n = 3$); different lowercase superscript letters within columns represent significant pairwise differences between forest types (Tukey's post hoc test, $P < 0.05$)

Fig. 2 Stem density (a) and basal area (b) of different forest types with respect to diameter size classes (DBH Class). Error bars denote one standard error ($n = 3$); different lowercase letters within each size class represent significant pairwise differences between forest types (Tukey's post hoc test, $P < 0.05$)



of basal area was similar to the pattern of stem density (Fig. 2b). CWM wood density of the four forest types significantly ($P < 0.01$) increased following the order: plantation < twice-logged forest < once-logged forest < old-growth forest, ranging from 0.377 ± 0.004 to 0.576 ± 0.013 g cm⁻³ (Table 2). The difference in CWM wood density of the four forest types can be attributed to the difference in distribution pattern of basal area in species-specific wood density classes (Fig. 3).

Changes in living biomass

TLB varied markedly among forest types ($P < 0.01$), from a minimum of 150.8 ± 4.6 Mg ha⁻¹ in the plantation to a maximum of 278.4 ± 1.5 Mg ha⁻¹ in the old-growth forest, with the twice-logged and once-logged forest intermediate (190.5 ± 12.8 and 217.6 ± 22.5 Mg ha⁻¹, respectively; Fig. 4a). Similarly, both AGB and CRB increased significantly along the disturbance gradient ($P < 0.01$; Fig. 4b, c). However, the highest FRB was observed in the plantation (5.99 ± 0.52 Mg ha⁻¹), which was slightly higher than that of twice-logged forest (5.52 ± 0.57 Mg ha⁻¹; $P = 0.94$) and significantly higher than that of once-logged (3.35 ± 0.19 Mg ha⁻¹; $P = 0.048$) and old-growth (3.37 ± 0.84 Mg ha⁻¹; $P = 0.049$; Fig. 4d) forests.

The plantation accumulated TLB at an average rate of 7.54 ± 0.23 Mg ha⁻¹ year⁻¹, slightly lower than the

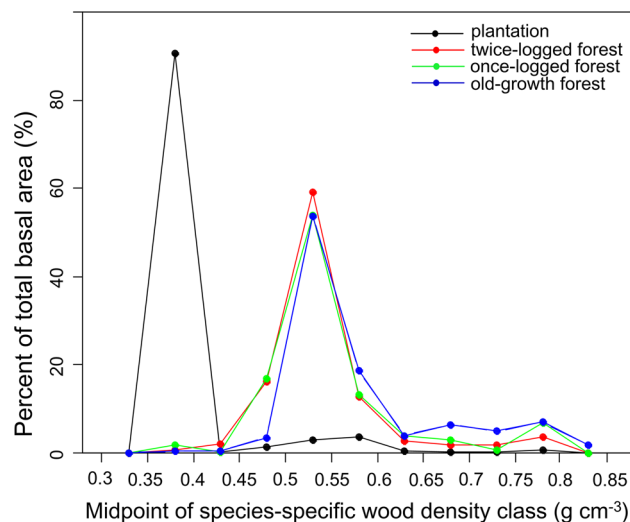


Fig. 3 Distribution pattern of basal area in species-specific wood density classes for the four forest types

recovery rate of the twice-logged forest (9.53 ± 0.64 or 8.73 ± 0.40 [adjusted] Mg ha⁻¹ year⁻¹; $P > 0.05$), but significantly higher than that of the once-logged forest (4.35 ± 0.45 Mg ha⁻¹ year⁻¹; $P = 0.005$; Table 3). Similar patterns were found for the average recovery rate of AGB and CRB (Table 3).

Multiple regressions show that, for TLB, AGB and CRB, only the basal area (DBH < 20 and DBH ≥ 20 cm) and CWM wood density were retained in the best-fit

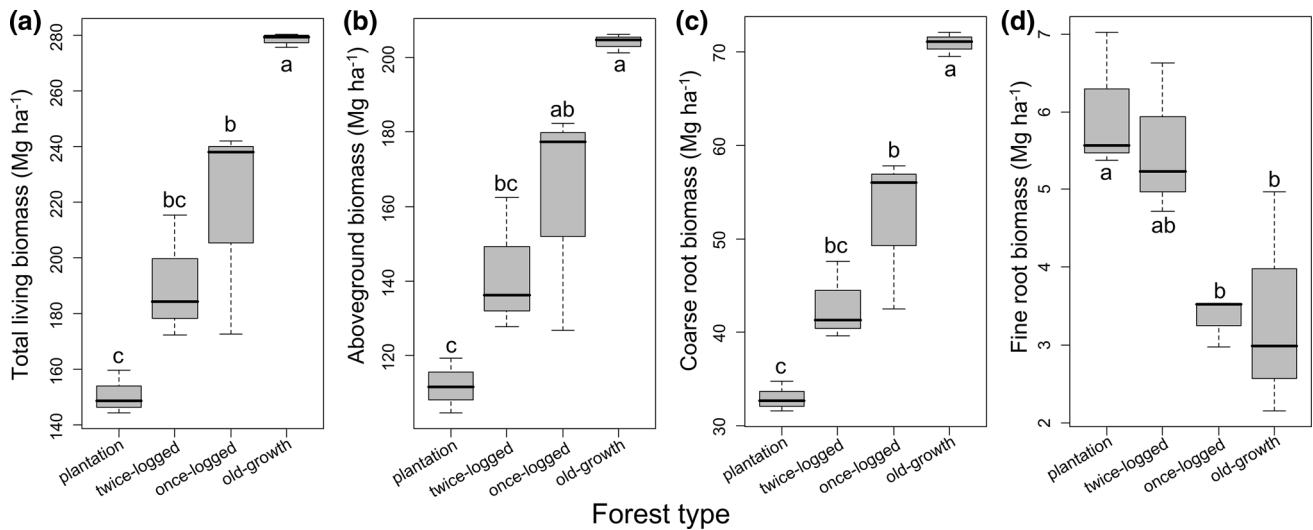


Fig. 4 Boxplot for living biomass of the four forest types in this study. For all forest types, $n = 3$; different lowercase letters represent significant pairwise differences between forest types (Tukey’s post

hoc test, $P < 0.05$); black lines in center of boxes are medians, whiskers show the range

Table 3 Average biomass recovery rate ($\text{Mg ha}^{-1} \text{ year}^{-1}$) since the last disturbance

Forest type	Total living biomass	Aboveground biomass	Coarse-root biomass
Plantation	$7.54^a \pm 0.23$	$5.59^a \pm 0.21$	$1.65^b \pm 0.05$
Twice-logged	$9.53^a \pm 0.64$	$7.11^a \pm 0.52$	$2.14^a \pm 0.12$
Twice-logged ^a	$8.73^a \pm 0.40$	$6.46^a \pm 0.32$	$1.99^{ab} \pm 0.08$
Once-logged	$4.35^b \pm 0.45$	$3.24^b \pm 0.36$	$1.04^c \pm 0.10$

Values are mean \pm SE ($n = 3$); different lowercase superscript letters within columns represent significant pairwise differences between forest types (Tukey’s post hoc test, $P < 0.05$)

^a Trees with DBH > 30 cm were excluded in the calculation

Table 4 Summary of the multiple regression analyses

Response variable	Model form	AICc	R ²	P value
Total living biomass (TLB)	$\text{TLB} = -318.9 + 5.5 \text{ BA} (<20 \text{ cm DBH}) + 8.1 \text{ BA} (\geq 20 \text{ cm DBH}) + 557.0 \rho$	94.68	0.988	<0.001
Aboveground biomass (AGB)	$\text{AGB} = -236.0 + 4.1 \text{ BA} (<20 \text{ cm DBH}) + 5.9 \text{ BA} (\geq 20 \text{ cm DBH}) + 414.2 \rho$	92.43	0.982	<0.001
Coarse-root biomass (CRB)	$\text{CRB} = -86.2 + 1.4 \text{ BA} (<20 \text{ cm DBH}) + 2.2 \text{ BA} (\geq 20 \text{ cm DBH}) + 141.0 \rho$	69.72	0.983	<0.001
Fine-root biomass (FRB)	$\text{FRB} = 8.462 + 0.0002 \text{ SD} (<20 \text{ cm DBH}) - 11.879 \rho$	40.18	0.751	0.002

Only the best-fit model with the lowest AICc (Akaike information criteria corrected for small sample size) was provided. All explanatory variables in the best-fit modes were significant at $P < 0.05$ level

BA, basal area; ρ , community-weighted mean wood density; SD, stem density

models, with 98.8, 98.2 and 98.3 % of the total variation explained, respectively (Table 4). Basal area of trees with DBH < 20 cm alone explained 10.6, 10.8 and 7.8 %, basal area of trees with DBH \geq 20 cm alone explained 35.5, 35.3 and 32.4 %, and CWM wood density alone explained 8.2, 8.4 and 6.2 %, of the total variation in TLB, AGB and CRB, respectively (Fig. 5). For FRB, only the stem density of trees with DBH < 20 cm and CWM wood density were retained, with 75.1 % of the total variation explained (Table 4). More than half of the explained variation was purely attributed to CWM wood density (39.5 % of total

variation), and 28.3 % purely attributed to stem density of trees with DBH < 20 cm (Fig. 5).

Discussion

Legacies of past disturbance on forest stand variables

Overall, the results of our comparison of the disturbed forests with the nearby undisturbed forests suggested that

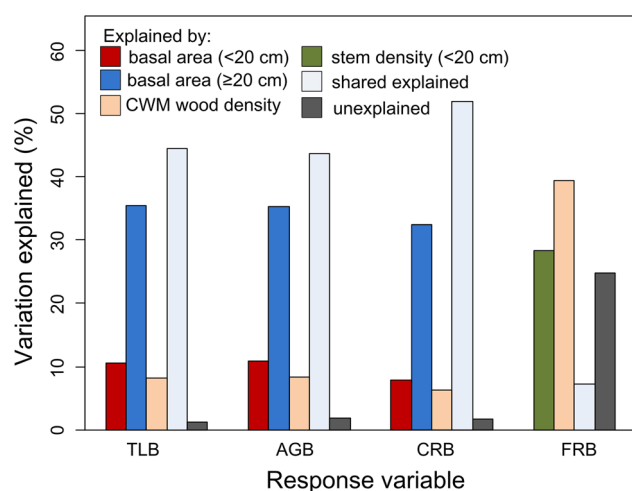


Fig. 5 Partial regression results show the percentage of variances in response variables (*TLB* total living biomass, *AGB* aboveground biomass, *CRB* coarse-root biomass, *FRB* fine-root biomass) explained by basal area (DBH < 20 and DBH ≥ 20 cm), community-weighted mean (CWM) wood density, stem density (DBH < 20 cm) independently and joint of them

legacies of past disturbance on stand variables were visible, especially in the plantation and twice-logged forest (Table 2; Fig. 2). The plantation was characterized by the extremely high stem density and basal area in size class of 10–20 cm (Fig. 2), reflecting the nature that most of the stems in the plantation belong to the same cohort and account for 95.4 ± 0.29 % of the total individuals in the size class of 10–20 cm. Significantly higher stem density and basal area in the smallest size class (1–10 cm DBH) of the twice-logged forest indicated that large number of trees have recruited following disturbance (Fig. 2). As indicated by the size distribution patterns of stem density and basal area (Fig. 2), the rapid recovery in basal area of the plantation was primarily driven by the fast growing rate of the planted tree species, whereas that of twice-logged forest was primarily driven by native tree recruitment and growth. Significant difference in stem density and basal area between once-logged and old-growth forests was still observed in the largest size class (DBH ≥ 30 cm; Fig. 2), suggesting that attaining a forest structure similar to undisturbed forests need more than 50 years.

CWM wood density changes significantly along the disturbance gradient (Table 2). This confirms that CWM trait value shows high sensitivity to disturbance (Carreño-Rocabado et al. 2012). Difference in CWM wood density among forest types can be attributed to difference in species composition and their relative dominance associated with human disturbance. In the plantation, most individuals were planted species, *C. lanceolata*, a fast-growing coniferous tree species with low-specific wood density (0.358 g cm^{-3}), resulting in the relative lower CWM wood

density (Table 2; Fig. 3). In natural forests, species composition and relative dominance gradually changed during recovery process, leading to increase in CWM wood density by decreasing the abundance and dominance of early-successional species with resource-acquisitive trait (lower wood density) and increasing the late-successional species with resource-conservative trait (higher wood density) (Ter Steege and Hammond 2001; Chave et al. 2006; Slik et al. 2008). Indeed, the percentage of basal area with wood density $<0.50 \text{ g cm}^{-3}$ decreased from 18.7 %, 18.9 % in twice-logged and once-logged forest, respectively, to 4.1 % in old-growth forest (Fig. 3). In contrast, the percentage of basal area with wood density $>0.60 \text{ g cm}^{-3}$ increased from 9.6 % in twice-logged forest to 14.1 % in once-logged forest and then to 23.6 % in old-growth forest, respectively (Fig. 3). Consistent with our result, Read and Lawrence (2003) reported that the weighted mean wood density was higher in mature forest than in secondary forest in dry tropical forest in Yucatan Peninsula. Similarly, Hector et al. (2011) found that average wood density of the selectively logged lowland dipterocarp forest was lower than that of nearby unlogged primary forest in Borneo. However, in wet tropical forests in southeast Mexico, Lohbeck et al. (2012) found that CWM wood density did not obviously changes with succession. This may partly due to the length of the chronosequence they observed is too short (3.3–24.6 years).

Biomass recovery following disturbance

Biomass increased rapidly following disturbance (Fig. 4). The plantation, twice-logged and once-logged forests recovered about 54.2, 68.4 and 78.1 % of TLB of the old-growth forest, respectively, in 20- to 50-year time frame, suggesting that these disturbed forests have notable ability to accumulate and store carbon. The AGB of natural forests estimated in our study is within the range of published AGB values of subtropical evergreen broad-leaved forests in China: 220.3 Mg ha^{-1} in a 24-ha old-growth forest dynamics monitoring plot near our study sites (Lin et al. 2012), 157.4 Mg ha^{-1} in a 52-year-old secondary forest in Tiantongshan in southeast China (Yang et al. 2010), 68.4 Mg ha^{-1} across Zhejiang province (ranging from 4.2 to 247.8 Mg ha^{-1} , encompassing both old-growth and secondary forests, calculated from Zhang et al. 2007), and 179.47 to $345.16 \text{ Mg ha}^{-1}$ in old-growth forests in Ailao Mountain, Yunnan province, southwest China (Liu et al. 2002). Estimating CRB is very difficult in forest because sampling plant roots at the stand level is destructive, laborious and technically challenging. For this reason, CRB was seldom accurately reported for subtropical evergreen broad-leaved forest in China in previous studies. Most of the published results were estimated by using root/shoot

ratio (e.g., Zhang et al. 2007; Lin et al. 2012). It has been reported that root/shoot ratios will change with climate, forest stand age, etc. (Mokany et al. 2006). So using the root/shoot ratios method may lead to biggish uncertainty in estimates of biomass (Peichl and Arain 2006). Consequently, our results will help to fill this information gap and could improve our ability to assess the role of below ground biomass carbon stock in the regional carbon balance. If we estimated CRB by using the root/shoot ratio of 0.23 (Fang et al. 1998), which was frequently used for the evergreen broad-leaved forests in subtropical China, this will lead to underestimates by 23.7, 28.5 and 33.8 % for the twice-logged, once-logged and old-growth forests, respectively. Biomass of Chinese fir plantation was well reported in the southern part of China (Wu 1984; Feng et al. 1999). AGB and CRB of the plantation in our study were similar to the magnitude of previous published values [AGB: $125.0 \pm 13.5 \text{ Mg ha}^{-1}$, CRB: $25.2 \pm 2.6 \text{ Mg ha}^{-1}$ (mean $\pm 1 \text{ SE}$, $n = 17$), stand age: 19–23 years, calculated from the data collected by Feng et al. 1999].

AGB average recovery rate of the once-logged forest ($3.24 \pm 0.36 \text{ Mg ha}^{-1} \text{ year}^{-1}$) was similar to the rate of a 52-year-old subtropical evergreen broad-leaved forest in eastern China ($3.03 \text{ Mg ha}^{-1} \text{ year}^{-1}$, calculated from Yang et al. 2010), which has similar species composition to the once-logged forest. The adjusted average recovery rate of AGB of the twice-logged forest ($6.46 \pm 0.32 \text{ Mg ha}^{-1} \text{ year}^{-1}$) in our study was similar to the global average recovery rate for tropical secondary forests on the first 20 years of succession ($6.2 \text{ Mg ha}^{-1} \text{ year}^{-1}$; Silver et al. 2000), and the value of $6.3 \pm 1.1 \text{ Mg ha}^{-1} \text{ year}^{-1}$ for a 20-year-old wet subtropical forest in Puerto Rico (Marin-Spiotta et al. 2007). However, these values were higher than those of dry tropical forests aged 5–29 years ($2.7\text{--}5.3 \text{ Mg ha}^{-1} \text{ year}^{-1}$; Vargas et al. 2008), and also higher than those of dry tropical forests aged 2–25 years ($2.3\text{--}3.4 \text{ Mg ha}^{-1} \text{ year}^{-1}$; Read and Lawrence 2003). The differences in recovery rate among studies were probably due to differences in species composition, land-use history and environmental conditions such as climate and substrate type among study sites.

Age-related decline of stand biomass accumulation was frequently reported in previous studies (Gower et al. 1996; Silver et al. 2000; Ryan et al. 2004; Marin-Spiotta et al. 2007; Vargas et al. 2008; Xu et al. 2012). For example, via reviewing the literatures, Silver et al. (2000) summarized that AGB had significantly faster accumulation rate during the first 20 years of recovery than the subsequent 60 years in tropical secondary forests. Conformably, in our study, average biomass recovery rate of the twice-logged forest, which suffered clear cut 50 years ago and high-intensive selective logging 20 years ago, was significantly higher than that of the 50 years old once-logged forest (Table 3), suggesting that biomass increased rapidly during the initial

phase of recovery, and then at a relatively slower rate. Possible mechanisms controlling age-related decline of stand biomass accumulation include forest production decline, tree mortality increase or their combination (Gower et al. 1996; Ryan et al. 2004; Xu et al. 2012).

We found only stand variables contributed to the variation in biomass over the disturbance gradient in our study area (Table 4). Basal area, especially the basal area of large trees ($\geq 20 \text{ cm DBH}$) which alone explained 35.5 % of the variation in TLB (Fig. 5), was most important to explain the variation in biomass over the disturbance gradient. This result is not surprising because diameter was used to estimate individual tree biomass, and strong linear relation between biomass and basal area was frequently reported (Baraloto et al. 2011). Many previous studies, conducted across a wide range of scales, have shown that stand-level wood density plays an important role in explaining spatial variation of forest biomass, for most studies with the positive relationships (Baker et al. 2004; Malhi et al. 2006; Baraloto et al. 2011; Quesada et al. 2012). In consistence, we found that CWM wood density positively and independently explained 8.2 % of the variation in TLB over the disturbance gradient (Table 4; Fig. 5). This suggests that, in addition to the changes in forest structure, changes in species composition as a result of past disturbances were also an important driver of biomass variation. Similarly, difference in biomass between disturbed and undisturbed forests causing by difference in species composition has been reported in a wet subtropical forest in Puerto Rico (Marin-Spiotta et al. 2007).

Fine root is the most important organ of plant for water and nutrient acquisition and is a major source of carbon in soil (Hendricks et al. 1993; Powers and Perez-Aviles 2013). In comparison with other stocks of biomass, changes in FRB during forest recovery process are more difficult to predict. Empirical results for FRB dynamics following disturbance remain inconsistent. For example, fine-root biomass has been reported to increase with stand age (Hertel et al. 2006; Varik et al. 2013), and some studies have reported hump-shaped relationship with stand age (Claud and George 2005; Peichl and Arain 2006; Borja et al. 2008; Yuan and Chen 2012), whereas other studies have found no relationship with stand age (Brearley 2011; Powers and Perez-Aviles 2013). These mixed results suggested that FRB is sensitive to changes in both biotic and abiotic environments (Yuan and Chen 2010). We found relatively higher FRB in the plantation and twice-logged forest than in the once-logged and old-growth forests (Fig. 4d). FRB over the disturbance gradient was best predicted positively by stem density of small trees ($\text{DBH} < 20 \text{ cm}$) and negatively by CWM wood density, with 75.1 % of the total variation explained and 28.3, 39.5 % independently attributed to stem density ($\text{DBH} < 20 \text{ cm}$) and CWM wood density,

respectively. Given that both lower in wood density and higher in stem density suggest relatively rapid forest dynamics (Guariguata and Ostertag 2001; Chave et al. 2009), our result can partly be explained by the optimal partitioning theory, i.e., plants allocate more biomass to belowground to maximize water and nutrient uptake that support fast tree growth (Bloom et al. 1985).

Implications for forest management

It is widely recognized that forest deforestation and degradation is a significant source of atmospheric CO₂, and recovering carbon stocks in disturbed forests to pre-disturbed level can contribute to climate change mitigation (Canadell and Raupach 2008; Mackey et al. 2013). In our study, if we assume that 50 % of biomass is carbon, this leads to estimates of biomass carbon stock of 75.4, 95.3 and 108.8 Mg ha⁻¹ in plantation, twice-logged and once-logged forests, respectively, compared with 139.2 Mg ha⁻¹ in old-growth forest, suggesting that at least 63.8, 43.95 and 30.4 Mg C ha⁻¹ could be sequestered by the plantation, twice-logged and once-logged forests, respectively, under the scenario that they completely recover to the level associated with the undisturbed old-growth forest. We can expect that forest structure can completely recover in specific period if they do not suffer from further disturbances (e.g., Chai and Tanner 2011). Complete recovery of forest biomass therefore depends on the regeneration of the pre-disturbed species composition, especially the regeneration of heavy-wood species. Consequently, we emphasize that species with high wood density and the areas with high CWM wood density demand special and prioritized attention to be protected in disturbed forests.

Chinese fir, an endemic species of China, is one of the most important plantation tree species in subtropical China, with a cultivation history of more than 1000 years (Wu 1984). According to the 7th National Forest Resources Inventory Report, by the end of 2008, Chinese fir plantations cover an area of 8.54 million hectares, accounting for about 13.8 and 4.37 % of total plantations and total forests areas of China, respectively (China State Forestry Administration 2009). Unfortunately, it has been reported that converting natural broad-leaved forests to Chinese fir plantation generally reduced forest biomass (Chen et al. 2005; Zhang et al. 2012; Chen et al. 2013). We also found that the Chinese fir plantation in our study site holds the highest basal area but lowest living biomass among the four forest types (Table 2; Fig. 4a). If these existing Chinese fir plantations are managed for sequestration of atmospheric CO₂, increasing CWM wood density is one of the effective strategies to approach the carbon carrying capacity—the mass of carbon stored in an ecosystem under natural regimes but excluding anthropogenic disturbance

(Gupta and Rao 1994; Keith et al. 2010). From a management perspective, restoration thinning (Dwyer et al. 2010), i.e., reducing the competition from the planted trees by cutting certain portion of them, and then, accelerating colonization by other broad-leaved tree species (generally with higher wood density than Chinese fir), should be encouraged.

Concluding remarks

In this study, to our knowledge, we provided the most comprehensive dataset to investigate the trajectories of China's subtropical forests recovery following different human disturbances to date. We found that: (1) 50 years is insufficient time for the forest structure and living biomass of clear-cut forest to recover to the values associated with undisturbed forest. (2) Average biomass recovery rates of subtropical forests in our study are comparable to the rates reported for some tropical forests of similar age. (3) CWM wood density was a strong predictor of variation in biomass over the disturbance gradient in addition to basal area. This result serve as a reminder that when managing disturbed forests for rehabilitating specific ecosystem functions, such as carbon storage, trait-based managing approach should not be overlooked. (4) If a place in subtropical China is designed for carbon sequestration, evergreen broad-leaved forest is more appropriate than Chinese fir plantation.

Acknowledgments We would like to thank Drs. Jianhua Chen, Xiaojuan Liu, Guoke Chen, Mr. Qi Jia and many undergraduate students from Zhejiang Normal University for their assistance with fieldwork. We are grateful to acknowledge the support of Earthwatch Institute and the HSBC Climate Partnership. This work was financially supported by the National Natural Science Foundation of China (NSFC31270496), the Strategic Priority Research Program of the Chinese Academy of Sciences (XDA05050204), the Fundamental Research Funds for the Central Universities (106112015CDJXY210012) and the 111 Project (B13041).

References

- Baker TR, Phillips OL, Malhi Y, Almeida S, Arroyo L, Di Fiore A, Erwin T, Killeen TJ, Laurance SG, Laurance WF, Lewis SL, Lloyd J, Monteagudo A, Neill DA, Patino S, Pitman NCA, Silva JNM, Martinez RV (2004) Variation in wood density determines spatial patterns in Amazonian forest biomass. *Glob Change Biol* 10:545–562
- Baraloto C, Rabaud S, Molto Q, Blanc L, Fortunel C, Herault B, Davila N, Mesones I, Rios M, Valderrama E, Fine PVA (2011) Disentangling stand and environmental correlates of above-ground biomass in Amazonian forests. *Glob Change Biol* 17:2677–2688
- Bloom AJ, Chapin FS, Mooney HA (1985) Resource limitation in plants—an economic analogy. *Annu Rev Ecol Syst* 16:363–392
- Borja I, De Wit HA, Steffenrem A, Majdi H (2008) Stand age and fine root biomass, distribution and morphology in a Norway spruce chronosequence in southeast Norway. *Tree Physiol* 28:773–784

- Brearley FQ (2011) Below-ground secondary succession in tropical forests of Borneo. *J Trop Ecol* 27:413–420
- Bunker DE, DeClerck F, Bradford JC, Colwell RK, Perfecto I, Phillips OL, Sankaran M, Naeem S (2005) Species loss and aboveground carbon storage in a tropical forest. *Science* 310:1029–1031
- Burnham KP, Anderson DR (2004) Model selection and multimodel inference: a practical information-theoretic approach, 2nd edn. Springer, New York
- Canadell JG, Raupach MR (2008) Managing forests for climate change mitigation. *Science* 320:1456–1457
- Carreño-Rocabado G, Peña-Claros M, Bongers F, Alarcón A, Licona J-C, Poorter L (2012) Effects of disturbance intensity on species and functional diversity in a tropical forest. *J Ecol* 100:1453–1463
- Chai SL, Tanner EVJ (2011) 150-year legacy of land use on tree species composition in old-secondary forests of Jamaica. *J Ecol* 99:113–121
- Chave J, Andalo C, Brown S, Cairns MA, Chambers JQ, Eamus D, Folster H, Fromard F, Higuchi N, Kira T, Lescure JP, Nelson BW, Ogawa H, Puig H, Riera B, Yamakura T (2005) Tree allometry and improved estimation of carbon stocks and balance in tropical forests. *Oecologia* 145:87–99
- Chave J, Muller-Landau HC, Baker TR, Easdale TA, Ter Steege H, Webb CO (2006) Regional and phylogenetic variation of wood density across 2456 neotropical tree species. *Ecol Appl* 16:2356–2367
- Chave J, Coomes D, Jansen S, Lewis SL, Swenson NG, Zanne AE (2009) Towards a worldwide wood economics spectrum. *Ecol Lett* 12:351–366
- Chazdon RL (2003) Tropical forest recovery: legacies of human impact and natural disturbances. *Perspect Plant Ecol Evol Syst* 6:51–71
- Chazdon RL, Letcher SG, van Breugel M, Martinez-Ramos M, Bongers F, Finegan B (2007) Rates of change in tree communities of secondary neotropical forests following major disturbances. *Philos Trans R Soc B* 362:273–289
- Chen WR (2000) Study on the net productivity dynamic changes of the above-ground portion of *Alniphyllum fortunei* plantation. *J Fujian For Technol* 27:31–34
- Chen GS, Yang YS, Xie JS, Guo JF, Gao R, Qian W (2005) Conversion of a natural broad-leaved evergreen forest into pure plantation forests in a subtropical area: effects on carbon storage. *Ann For Sci* 62:659–668
- Chen QQ, Xu WQ, Li SG, Fu SL, Yan JH (2013) Aboveground biomass and corresponding carbon sequestration ability of four major forest types in south China. *Chin Sci Bull* 58:1551–1557
- China State Forestry Administration (2009) China forest resources report—the 7th National Forest Inventory. China Forestry Publishing House, Beijing
- Claus A, George E (2005) Effect of stand age on fine-root biomass and biomass distribution in three European forest chronosequences. *Can J For Res* 35:1617–1625
- Condit R (1998) Tropical forest census plots. Springer, New York
- Conti G, Díaz S (2013) Plant functional diversity and carbon storage—an empirical test in semi-arid forest ecosystems. *J Ecol* 101:18–28
- Díaz S, Lavorel S, de Bello F, Quétier F, Grigulis K, Robson M (2007) Incorporating plant functional diversity effects in ecosystem service assessments. *Proc Natl Acad Sci USA* 104:20684–20689
- Du S, Gao X (2006) Soil analysis technology specification. China Agriculture Press, Beijing
- Du G, Hong L, Yao G (1987) Estimate and analysis the aboveground biomass of a secondary evergreen broad-leaved forest in Northwest of Zhejiang. *J Zhejiang For Sci Technol* 7:5–12
- Dwyer JM, Fensham R, Buckley YM (2010) Restoration thinning accelerates structural development and carbon sequestration in an endangered Australian ecosystem. *J Appl Ecol* 47:681–691
- Editorial Group of Forestry Chorography in Kaihua County (1988) Forestry chorography in Kaihua County. Zhejiang People's Publishing House, Hangzhou
- Fang JY, Wang GG, Liu G, Xu S (1998) Forest biomass of China: an estimate based on the biomass–volume relationship. *Ecol Appl* 8:1084–1091
- Fang JY, Chen AP, Peng CH, Zhao SQ, Ci L (2001) Changes in forest biomass carbon storage in China between 1949 and 1998. *Science* 292:2320–2322
- FAO (2010) Global forest resources assessment 2010. Food and Agriculture Organization of the United Nations, Rome
- Feng ZW, Wang XK, Wu G (1999) Biomass and productivity in forest ecosystems. China Science Press, Beijing
- Gower ST, McMurtrie RE, Murty D (1996) Aboveground net primary production decline with stand age: potential causes. *Trends Ecol Evol* 11:378–382
- Guariguata MR, Ostertag R (2001) Neotropical secondary forest succession: changes in structural and functional characteristics. *For Ecol Manag* 148:185–206
- Gupta RK, Rao DLN (1994) Potential of wastelands for sequestering carbon by reforestation. *Curr Sci* 66:378–380
- Hector A, Philipson C, Saner P, Chamagne J, Dzikiffi D, O'Brien M, Snaddon JL, Ulok P, Weilenmann M, Reynolds G, Godfray H CJ (2011) The Sabah biodiversity experiment: a long-term test of the role of tree diversity in restoring tropical forest structure and functioning. *Philos Trans R Soc B* 366:3303–3315
- Hendricks JJ, Nadelhoffer KJ, Aber JD (1993) Assessing the role of fine roots in carbon and nutrient cycling. *Trends Ecol Evol* 8:174–178
- Hertel D, Hölscher D, Köhler L, Leuschner C (2006) Changes in fine root system size and structure during secondary succession in a Costa Rican montane oak forest. In: Kappelle M (ed) Ecology and conservation of neotropical montane oak forests. Springer, Berlin, pp 283–297
- Houghton RA (2007) Balancing the global carbon budget. *Annu Rev Earth Pl Sc* 35:313–347
- Keith H, Mackey B, Berry S, Lindenmayer D, Gibbons P (2010) Estimating carbon carrying capacity in natural forest ecosystems across heterogeneous landscapes: addressing sources of error. *Glob Change Biol* 16:2971–2989
- Kira T (1991) Forest ecosystems of east and Southeast Asia in a global perspective. *Ecol Res* 6:185–200
- Lai JS, Yang B, Lin DM, Kerckhoff AJ, Ma KP (2013) The allometry of coarse root biomass: log-transformed linear regression or nonlinear regression? *PLoS ONE* 8:e77007
- Legendre P, Legendre L (2003) Numerical ecology, 2nd edn. Elsevier, New York
- Letcher SG, Chazdon RL (2009) Rapid recovery of biomass, species richness, and species composition in a forest chronosequence in northeastern Costa Rica. *Biotropica* 41:608–617
- Li WH (2004) Degradation and restoration of forest ecosystems in China. *For Ecol Manag* 201:33–41
- Li N, Xu WB, Lai JS, Yang B, Lin DM, Ma KP (2013) The coarse root biomass of eight common tree species in subtropical evergreen forest. *Chin Sci Bull* 58:329–335
- Lin DM, Lai JS, Muller-Landau HC, Mi XC, Ma KP (2012) Topographic variation in aboveground biomass in a subtropical evergreen broad-leaved forest in China. *PLoS ONE* 7:e48244
- Liu WY, Fox JED, Xu ZF (2002) Biomass and nutrient accumulation in montane evergreen broad-leaved forest (*Lithocarpus xylocarpus* type) in Ailao Mountains, SW China. *For Ecol Manag* 158:223–235

- Liu XJ, Swenson NG, Wright SJ, Zhang LW, Song K, Du YJ, Zhang JL, Mi XC, Ren HB, Ma KP (2012) Covariation in plant functional traits and soil fertility within two species-rich forests. *PLoS ONE* 7:e34767
- Lohbeck M, Poorter L, Pazb H, Plac L, Breugeld MV, Martínez-Ramos M, Bongers F (2012) Functional diversity changes during tropical forest succession. *Perspect Plant Ecol Evol Syst* 14:89–96
- Lou LF, Jin SH (2000) Spermatophyta flora of Gutianshan Nature Reserve in Zhejiang. *J Beijing For Univ* 22:33–39
- Mackey B, Prentice IC, Steffen W, House JI, Lindenmayer D, Keith H, Berry S (2013) Untangling the confusion around land carbon science and climate change mitigation policy. *Nat Clim Change* 3:552–557
- Malhi Y, Wood D, Baker TR, Wright J, Phillips OL, Cochrane T, Meir P, Chave J, Almeida S, Arroyo L, Higuchi N, Killeen TJ, Laurance SG, Laurance WF, Lewis SL, Monteagudo A, Neill DA, Vargas PN, Pitman NCA, Quesada CA, Salomao R, Silva JNM, Lezama AT, Terborgh J, Martinez RV, Vinceti B (2006) The regional variation of aboveground live biomass in old-growth Amazonian forests. *Glob Change Biol* 12:1107–1138
- Marin-Spiotta E, Ostertag R, Silver WL (2007) Long-term patterns in tropical reforestation: plant community composition and aboveground biomass accumulation. *Ecol Appl* 17:828–839
- Martin PA, Newton AC, Bullock JM (2013) Carbon pools recover more quickly than plant biodiversity in tropical secondary forests. *Proc R Soc B: Biol Sci* 280:20132236
- Millennium Ecosystem Assessment (MEA) (2005) Ecosystems and human well-being: synthesis. Island Press, Washington, DC
- Mokany K, Raison RJ, Prokushkin AS (2006) Critical analysis of root: shoot ratios in terrestrial biomes. *Glob Change Biol* 12:84–96
- Muller-Landau HC (2004) Interspecific and inter-site variation in wood specific gravity of tropical trees. *Biotropica* 36:20–32
- Oliveira MDRG, Noordwijk MV, Gaze SR, Brouwer G, Bona S, Mosca G, Hairiah K (2000) Auger sampling, ingrowth cores and pinboard methods. Springer, Berlin
- Pan Y, Birdsey RA, Fang J, Houghton R, Kauppi PE, Kurz WA, Phillips OL, Shvidenko A, Lewis SL, Canadell JG, Ciais P, Jackson RB, Pacala SW, McGuire AD, Piao S, Rautiainen A, Sitch S, Hayes D (2011) A large and persistent carbon sink in the world's forests. *Science* 333:988–993
- Peichl M, Arain AA (2006) Above- and belowground ecosystem biomass and carbon pools in an age-sequence of temperate pine plantation forests. *Agric For Meteorol* 140:51–63
- Piao SL, Fang JY, Ciais P, Peylin P, Huang Y, Sitch S, Wang T (2009) The carbon balance of terrestrial ecosystems in China. *Nature* 458:1009–1013
- Powers JS, Perez-Aviles D (2013) Edaphic factors are a more important control on surface fine roots than stand age in secondary tropical dry forests. *Biotropica* 45:1–9
- Quesada CA, Phillips OL, Schwarz M, Czimczik CI, Baker TR, Patino S, Fyllas NM, Hodnett MG, Herrera R, Almeida S, Davila EA, Arneeth A, Arroyo L, Chao KJ, Dezzee N, Erwin T, di Fiore A, Higuchi N, Coronado EH, Jimenez EM, Killeen T, Lezama AT, Lloyd G, Lopez-Gonzalez G, Luizao FJ, Malhi Y, Monteagudo A, Neill DA, Vargas PN, Paiva R, Peacock J, Penuela MC, Cruz AP, Pitman N, Priante N, Prieto A, Ramirez H, Rudas A, Salomao R, Santos AJB, Schmerler J, Silva N, Silveira M, Vasquez R, Vieira I, Terborgh J, Lloyd J (2012) Basin-wide variations in Amazon forest structure and function are mediated by both soils and climate. *Biogeosciences* 9:2203–2246
- Read L, Lawrence D (2003) Recovery of biomass following shifting cultivation in dry tropical forests of the Yucatan. *Ecol Appl* 13:85–97
- Ryan MG, Binkley D, Fownes JH, Giardina CP, Senock RS (2004) An experimental test of the causes of forest growth decline with stand age. *Ecol Monogr* 74:393–414
- Silver WL, Ostertag R, Lugo AE (2000) The potential for carbon sequestration through reforestation of abandoned tropical agricultural and pasture lands. *Restor Ecol* 8:394–407
- Slik JWF, Bernard CS, Breman FC, Van Beek M, Salim A, Sheil D (2008) Wood density as a conservation tool: quantification of disturbance and identification of conservation-priority areas in tropical forests. *Conserv Biol* 22:1299–1308
- Ter Steege H, Hammond DS (2001) Character convergence, diversity, and disturbance in tropical rain forest in Guyana. *Ecology* 82:3197–3212
- Vargas R, Allen MF, Allen EB (2008) Biomass and carbon accumulation in a fire chronosequence of a seasonally dry tropical forest. *Glob Change Biol* 14:109–124
- Varik M, Aosaar J, Ostonen I, Lõhmus K, Uri V (2013) Carbon and nitrogen accumulation in belowground tree biomass in a chronosequence of silver birch stands. *For Ecol Manag* 302:62–70
- Wang XH, Kent M, Fang XF (2007) Evergreen broad-leaved forest in Eastern China: its ecology and conservation and the importance of resprouting in forest restoration. *For Ecol Manag* 245:76–87
- Wu Z (1980) The vegetation of China. Science Press, Beijing
- Wu ZL (1984) Chinese fir. China Forestry Publishing House, Beijing
- Xu C-Y, Turnbull MH, Tissue DT, Lewis JD, Carson R, Schuster WSF, Whitehead D, Walcroft AS, Li J, Griffin KL (2012) Age-related decline of stand biomass accumulation is primarily due to mortality and not to reduction in NPP associated with individual tree physiology, tree growth or stand structure in a Quercus-dominated forest. *J Ecol* 100:428–440
- Xu Y, Lin D, Mi X, Ren H, Ma K (2014) Recovery dynamics of secondary forests with different disturbance intensity in the Gutianshan National Nature Reserve. *Biodivers Sci* 22:358–365
- Yang TH, Song K, Da LJ, Li XP, Wu JP (2010) The biomass and aboveground net primary productivity of *Schima superba*–*Castanopsis carlesii* forests in east China. *Sci China Life Sci* 53:811–821
- Yu MJ, Hu ZH, Yu JP, Ding BY, Fang T (2001) Forest vegetation types in Gutianshan National Natural Reserve in Zhejiang. *J Zhejiang Univ (Agric Life Sci)* 27:375–380
- Yuan ZY, Chen HYH (2010) Fine root biomass, production, turnover rates, and nutrient contents in boreal forest ecosystems in relation to species, climate, fertility, and stand age: literature review and meta-analyses. *Crit Rev Plant Sci* 29:204–221
- Yuan ZY, Chen HYH (2012) Fine root dynamics with stand development in the boreal forest. *Funct Ecol* 26:991–998
- Zhang J, Ge Y, Chang J, Jiang B, Jiang H, Peng CH, Zhu JR, Yuan WG, Qi LZ, Yu SQ (2007) Carbon storage by ecological service forests in Zhejiang Province, subtropical China. *For Ecol Manag* 245:64–75
- Zhang GB, Li XQ, Xu ZH, Hu CQ, Zhang SN, Hu GH (2012) Analysis of the carbon stock structure in forest plantations with different regeneration methods. *Ecol Environ Sci* 21:206–212